Electrical transport in a two-dimensional electron and hole gas on a Si(001)-(2×1) surface

Hassan Raza,[1] Tehseen Z. Raza,[2] and Edwin C. Kan[1]
[1]*School of Electrical and Computer Engineering, Cornell University, Ithaca, New York 14853, USA*
[2]*School of Electrical and Computer Engineering, Purdue University, West Lafayette, Indiana 47907, USA*
(Received 1 April 2008; revised manuscript received 14 September 2008; published 6 November 2008)

Si(001)-(2×1) surface is one of the many two-dimensional systems of scientific and applied interest. Due to its asymmetric dimer reconstruction, transport through this surface can be considered in two distinct directions, i.e., along and perpendicular to the paired dimer rows. We calculate the zero-bias conductance of these surface states under flatband condition and find that conduction along the dimer row direction is significant due to strong orbital hybridization. Additionally, we find that the surface conductance is orders of magnitude higher than the bulk conductance close to the band edges for the unpassivated surface at room temperature. Thus, we propose that the transport through these surface states may be the dominant conduction mechanisms in the recently reported scanning tunneling microscopy of silicon nanomembranes. The zero-bias conductance is also calculated for the weakly interacting dangling-bond wires along and perpendicular to the dimer row direction and similar trends are obtained. The extended Hückel theory is used for the electronic structure calculations.

DOI: 10.1103/PhysRevB.78.193401 PACS number(s): 73.20.−r, 73.40.−c, 73.63.−b

I. INTRODUCTION

Two-dimensional (2D) electronic systems[1] have been of great interest. In metal-oxide-semiconductor (MOS) technology,[2] the 2D electron and hole gases are the key for functioning of the modern integrated circuits.[3] Graphene is another noteworthy example of 2D transport and has attracted tremendous interest recently.[4]

The electronic structure of the Si(001) surface has been a topic of study for decades due to its scientific and applied interest. Although, some aspects of this particular surface are still controversial, overall it is well understood.[5,6] An unpassivated Si surface with paired asymmetric dimer (AD) reconstruction introduces two surface bands which have a 2D character.[5,6] The band corresponding to the antibonding state (π^* band) has acceptor states.[2] Similarly, the band corresponding to the bonding state (π band) has donor states.[2] These π^* and π states are localized on the bottom and top dimer atoms, respectively.[5] The surface-state density is about 10^{15} cm^{-2} for π^* and π bands. Since the π^* band is fully unoccupied and the π band is fully occupied, they do not contribute to the transport in the absence of doping and surface band bending.

These two bands, however, may start conducting with doping and/or surface band bending. In such a scenario, the transport through the π^* and π bands can be thought of as electron and hole transports, respectively. Recently, Zhang *et al.*[7] reported scanning tunneling microscopy (STM) of 10-nm-thick silicon nanomembranes with about 10^{15} cm^{-3} *p*-type doping. With the atomic resolution for this system in STM, they proposed that surface doping enabled by thermal excitation of electrons in π^* band results in holes in the valence band, which enables the hole conduction inside the valence band. Zhang *et al.*[7] placed the π band edge a few tenths of an electron volt below the valence-band edge. We find that after summation over the transverse Brillouin zone, the bottom of the π^* band lies about 0.4 eV below the conduction-band edge (E_c) and the top of the π band lies about 0.2 eV above the valence-band edge (E_v). Additionally, our model predicts that the zero-bias conductance through these surface states is at least 3 orders of magnitude higher than that of the bulk, with the same doping as used in STM (Ref. 7) for a 1-nm-thick nanomembrane. Thus, we propose that the surface-state transport alone may be the dominant conductance mechanism in silicon nanomembranes. In contrast, a 10-nm-thick nanomembrane can possibly give an order of magnitude higher bulk conduction. However, the surface conduction would be about 2 orders of magnitude higher and hence would still be the dominant mechanism.

We calculate the transmission and the zero-bias conductance under flatband condition for these surface states in directions parallel and perpendicular to the dimer row, referred to as $[\bar{1}10]$ and [110], respectively. We also calculate transmission and zero-bias conductance under flatband condition for paired dangling-bond (DB) wires separated by hydrogenated DB wires in the above-mentioned directions.

II. MODEL SYSTEMS

In a previous study,[8] we report that an isolated unpaired DB on an otherwise perfectively hydrogenated Si(001) surface will only affect its neighboring Si atoms within 10 Å. Same is the case for the paired DBs on the Si surface.[6] The π^* and π states, respectively, are localized on the bottom and top Si atoms in the paired AD. In the $[\bar{1}10]$ direction, the Si dimer atoms on which the π^* and π states are localized, are only 3.84 Å apart, while in the [110] direction, they are about 7.68 Å apart. This hybridization anisotropy in $[\bar{1}10]$ and [110] directions results in different bandwidths.[6] Apart from this, the extent of the wave-function overlap of these surface states also affects the transport in these directions.

In this Brief Report, we consider five model systems for the transport calculations as described in Table I and Fig. 1. The transport direction is shown by the arrows, and the unit cell used for each model is shown by the dashed lines. Model I is a hydrogenated surface and is expected to have bulk Si band gap for a 16 layer unit cell. We calculate transmission

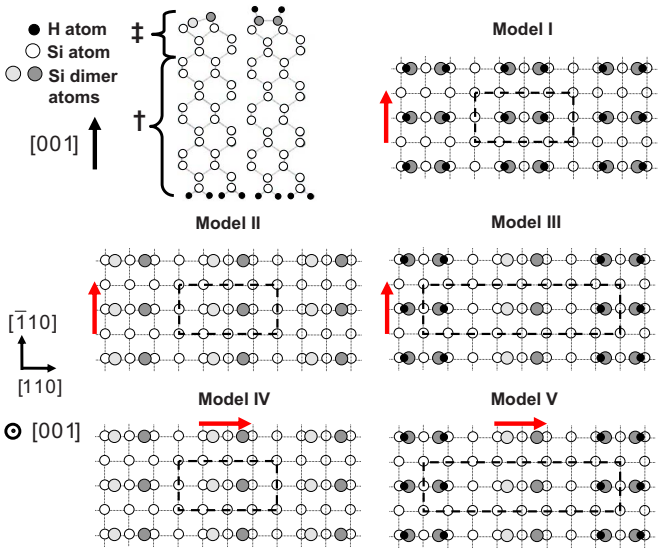

FIG. 1. (Color online) Ball and stick models. Unpassivated paired AD surface and hydrogenated symmetric dimer surface. Top four layers, represented by ‡, are relaxed due to surface reconstruction. Bottom 12 layers, represented by †, are bulk layers. The back surface is hydrogenated to eliminate any inadvertent DB induced states. The top Si atom of the AD surface is shaded as black and the bottom Si atom is shaded as gray. The atoms below the first monolayer of Si surface are represented by white circles. The direction parallel to the dimer row is referred to as $[\bar{1}10]$, whereas the one perpendicular to the dimer row is labeled as [110]. Atomic coordinates for these structures are discussed and reported in Ref. 6. Atomic visualization is done using GAUSSVIEW (Ref. 9).

for this model in $[\bar{1}10]$ direction and use it as a reference for the other models. Models II and IV are unpassivated surfaces and the transport is calculated in the $[\bar{1}10]$ and the [110] directions, respectively. Models III and V are paired DB wires separated by hydrogenated wires, and transport is calculated in the $[\bar{1}10]$ and the [110] directions, respectively. The size of the unit cell used and number of atoms per unit cell are also given in Table I. Since DBs interact within 10 Å,[6] enough neighboring unit cells are included to ensure that adjacent DBs are isolated while calculating the Hamiltonian (H) and the overlap (S) matrices for the $E(\vec{k})$ calculations.

TABLE I. Details of the model systems. The models consist of 16 atomic layers shown in Fig. 1 to eliminate quantization effects and hence to obtain bulk Si band gap. The total number of Si atoms (excluding H atoms on top and back surfaces) per unit cell is also given. As shown in Fig. 1(a) (2×1) unit cell has two repeating unit cells in the [110] direction (perpendicular to dimer row) and one unit cell in the $[\bar{1}10]$ direction (along dimer row).

Model	Unit cell surface	Unit cell[a]	Atoms[b]
I	H:Si(001)-(2×1)	2×1	16
II	Si(001)-(2×1)-AD [c]	2×1	16
III	Paired dangling-bond wire[c]	4×1	32
IV	Si(001)-(2×1)-AD [d]	2×1	16
V	Paired dangling-bond wire[d]	4×1	32

[a]Multiples of 3.84 Å-lattice constant of bulk unit cell.
[b]Number of Si atoms only per unit cell.
[c]In $[\bar{1}10]$ direction.
[d]In [110] direction.

III. THEORETICAL CALCULATIONS

We use the extended Hückel theory (EHT) for the electronic structure calculations as in Ref. 6. EHT prescribes a semiempirical tight-binding procedure using a Slater-type orbital nonorthogonal basis set. For Si, EHT is benchmarked[10] with the GW approximation and gives the correct band-structure features, such as band offsets and dispersions. Transferable EHT parameters used in this Brief Report are taken from Ref. 10 and are summarized in Table II. We use one orbital $(1s)$ basis set for the H atom, whereas a nine-orbital $(3s, 3p,$ and $3d)$ basis set is used for the Si atom.

In order to calculate the transport properties for a 2D channel, we calculate the $E(k)$ diagrams over the transverse Brillouin zone for each wave vector in the transverse direction $(k_\parallel)$ by transforming the real-space Hamiltonian (H) and overlap (S) matrices to reciprocal $(\vec{k})$ space;

$$H(\vec{k}) = \sum_{m=1}^{N} H_{mn} e^{i\vec{k}\cdot(\vec{d_m}-\vec{d_n})}, \tag{1}$$

$$S(\vec{k}) = \sum_{m=1}^{N} S_{mn} e^{i\vec{k}\cdot(\vec{d_m}-\vec{d_n})}, \tag{2}$$

where $\vec{k}=(k_\parallel,k_t)-k_t$ is the wave vector in the transport direction. For each transverse wave vector $(k_\parallel)$, the system thus becomes one-dimensional (1D), and hence its transmission is independent of the dispersion. This enables transmission to be calculated numerically by counting band crossings at a particular energy for each transverse $k_\parallel$. Finally transmission per unit length is calculated by summation over transverse $k_\parallel$ as follows:

$$T(E) = \frac{1}{L}\sum_{k_\parallel} \tilde{T}(E_l,k_\parallel) = \frac{1}{2\pi}\int dk_\parallel \tilde{T}(E_l,k_\parallel). \tag{3}$$

The zero-bias conductance (G_o) under flatband condition at a finite temperature is then calculated as follows (see Appendix):

$$G_o = \frac{2q^2}{h}\frac{1}{kT}\int dET(E)\frac{e^{(E-\mu_o)/kT}}{[1+e^{(E-\mu_o)/kT}]^2}. \tag{4}$$

The same result is valid for the zero-bias differential conductance as well.

IV. DISCUSSION OF RESULTS

We report the transmission per unit transverse length through model I in Fig. 2, which shows a clean bulk band gap of 1.18 eV as expected due to the hydrogen passivation. We use it as a reference for the calculations of other model systems. For the AD surface (model II), transmission through

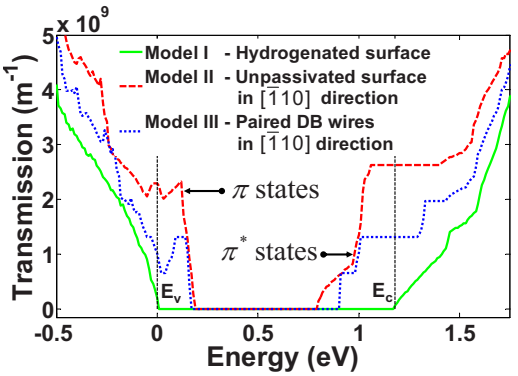

FIG. 2. (Color online) Transmission calculations for models I, II, and III. Hydrogenated Si(001) surface (model I) gives bulk Si band gap of 1.18 eV. Unpassivated Si(001) surface (model II) gives large transmission in the dangling-bond row direction ($[\bar{1}10]$) for both the π^* and the π states because the dimer atoms on which these states are localized are 3.84 Å apart. Transmission through the paired dangling-bond (model III) wire along the dangling-bond row direction, is about half of that in model II due to half of the total dangling-bond states per unit transverse length.

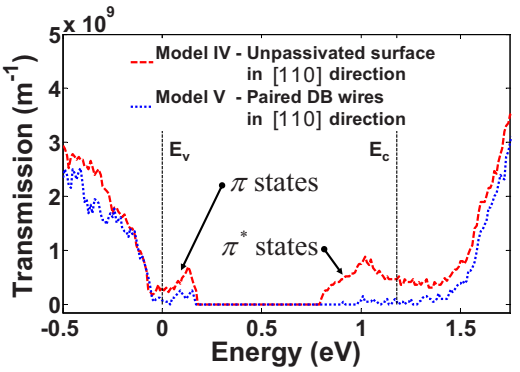

FIG. 3. (Color online) Transmission calculations for models IV and V. For model IV, the transmission through Si surface states in the direction perpendicular to dimer row direction ([110]) is smaller than the one along the dimer row direction (model II) due to the reduced hybridization between surface states—DB atoms being 7.68 Å apart. The conclusion for the DB wire, for which the transmission is calculated perpendicular to dimer row direction (model V), is the same.

the π^* and π states is shown in Fig. 2 along the $[\bar{1}10]$ direction. The atoms are 3.84 Å apart on which π^* and π states are localized. Since wave functions are extended up to 10 Å, hybridization is strong and hence the transmission is large. The transmission through the π^* state starts increasing about 0.4 eV below the conduction-band edge. The corresponding zero-bias conductance under flatband condition is calculated using Eq. (4) and is shown in Fig. 4. The maximum transmission through the π^* state is about 3×10^9/m, which gives a zero-bias conductance of about 0.2 S/μm. Additionally, the transmission through the π state is about 0.2 eV above the valence-band edge. For model III, the transmission is again large because atoms corresponding to π^* and π states are 3.84 Å apart. But since the overall density of dangling bond is half as that of model II, the transmission is almost half for both the states. On the other hand, there are some differences in characteristic features due to varying band offsets at various transverse wave vectors ($k_{\|}$) for models II and III.

Models IV and V are the same as models II and III, but the transmission is calculated in the [110] direction. As shown in Fig. 3, the overall transmission is smaller even inside the conduction and the valence bands because in this direction Si atoms in the top four surface layers are further apart due to the asymmetric reconstruction. Apart from this for model IV, since the Si atoms where the π^* and π states are localized are now 7.68 Å apart, there is small hybridization and hence the surface-state hopping is quenched. The maximum transmission inside the band gap for model IV is about 0.75×10^9/m, which gives a conductance of about 0.05 S/m. For model V, the unpassivated bottom and top dimer atoms in the transport direction are about 15.36 Å apart, which results in even smaller hybridization of the π^* and the π states. Therefore, the transmission through these states for model V is much smaller.

TABLE II. EHT parameters used for H and Si atoms. $K_{\mathrm{EHT}}=2.3$.

Orbital	$E_{\text{on-site}}$ (eV)	C_1	C_2	ξ_1 (Å^{-1})	ξ_2 (Å^{-1})
H:1s	−16.151 80	0.535 58		0.885 60	
Si:3s	−18.102 64	0.703 66		1.836 11	
Si:3p	−11.252 98	0.027 70	0.983 13	0.789 01	1.709 88
Si:3d	−5.347 060	0.683 83	0.469 50	0.682 92	1.721 02

The calculated zero-bias conductance under flatband condition at room temperature is shown on a linear and a logarithmic scale in Fig. 4. The conductance for models II and III is orders of magnitude higher than that of model I inside the band gap. For model IV, the conductance is about 2 orders of magnitude higher for the π^* states and less than 1 order of magnitude higher for the π states than that of model V. Furthermore, the zero-bias conductance decreases exponentially inside the band gap due to the Fermi tail. For the experimental conditions used in Ref. 7, the band bending is small, and hence based on our flatband zero-bias conductance calculations, we propose that the surface-state hoping is the dominant conduction mechanism in the recently reported STM of lightly doped silicon nanomembranes.[7]

In these calculations, we have assumed that the transport is coherent and the channel is in the ballistic regime. The transmission is thus independent of the channel length. The results reported provide an upper limit of transmission and conductance for these surface states. In this Brief Report, effects of gate voltage and realistic contacts are ignored. In Ref. 11, we provide the basic formalism to perform these calculations. Furthermore, we leave the role of defects, the electrostatic effects of the dopant atoms and dephasing due to electron-phonon scattering for future work. Interestingly, it has been suggested that atomic steps on Si(111) surface can decrease conduction by 2 orders of magnitude[12] through the surface states.

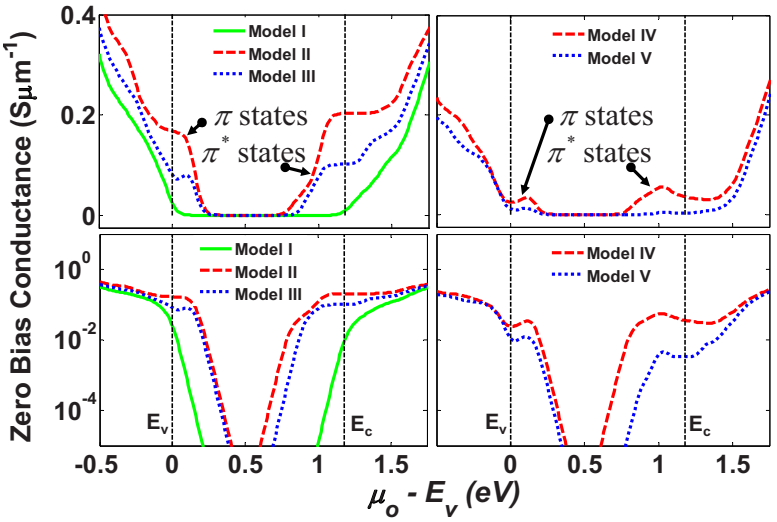

FIG. 4. (Color online) Zero-bias conductance under flatband condition. For model I (hydrogenated surface with transport in the dimer row direction), the conductance decreases exponentially inside the band gap due to Fermi tail. Close to the band edge, the zero-bias conductance is orders of magnitude higher for model II (unpassivated surface with transport in dimer row direction) than that of model I. The zero-bias conductance for model III (DB wire with transport in dimer row direction) follows the same trend as that of model II with some quantitative differences. The zero-bias conductance for the π^* states of model IV (unpassivated surface with transport perpendicular to the dimer row direction) is 2 orders of magnitude higher and less than 1 order of magnitude higher than that of model V (DB wire with transport perpendicular to the dimer row direction) inside the band gap.

V. CONCLUSIONS

We have studied the transport through Si(001)-(2×1) surface states with asymmetric dimer reconstruction in the dimer row and its perpendicular direction. We find significant transmission in the dimer row direction due to strong hybridization between dangling bonds being 3.84 Å apart. However, in the direction perpendicular to the dimer row, bottom and top dimer atoms on which π^* and π states are localized are about 7.68 Å apart. Their hybridization is thus weak. We find similar trends for the paired dangling-bond wires. Apart from this, the zero-bias conductance under flatband condition at room temperature around the band edges is at least 3 orders of magnitude higher for these surface states in comparison with that of passivated surface. Therefore, we propose that conduction through the surface states may be the dominant conduction mechanism in the recently reported scanning tunneling microscopy results of silicon nanomembranes on insulator.

ACKNOWLEDGMENTS

We thank M. G. Lagally and A. Alam for useful discussions. The work was supported by National Science Foundation (NSF) and by Nanoelectronics Research Institute (NRI) through Center for Nanoscale Systems (CNS) at Cornell University.

APPENDIX

We derive Eq. (4) as follows. Starting with the Landaüer's approach,

$$I = \frac{2q}{h}\int dET(E)(f_1 - f_2).$$

For $|qV| \ll kT$, using Taylor series expansion and retaining the first term for $e^{qV/kT}$, it can be shown that

$$f_1 - f_2 = \frac{qV}{kT}\frac{e^{(E-\mu_o)/kT}}{[1+e^{(E-\mu_o)/kT}]^2}.$$

[1] T. Ando, A. B. Fowler, and F. Stern, Rev. Mod. Phys. **54**, 437 (1982).
[2] S. M. Sze, *Physics of Semiconductor Devices* (Wiley-Interscience, New York, 1981).
[3] Y. Taur and T. H. Ning, *Fundamentals of Modern VLSI Devices* (Cambridge University Press, Cambridge, UK, 1998).
[4] A. K. Geim and K. S. Novoselov, Nature Mater. **6**, 183 (2007).
[5] G. P. Srivastava, *Theoretical Modelling of Semiconductor Surfaces* (World Scientific, New Jersey, 1999).
[6] H. Raza, Phys. Rev. B **76**, 045308 (2007), and references therein.
[7] P. Zhang, E. Tevaarwerk, B.-N. Park, D. E. Savage, G. K. Celler, I. Knezevic, P. G. Evans, M. A. Eriksson, and M. G. Lagally, Nature (London) **439**, 703 (2006).
[8] H. Raza, K. H. Bevan, and D. Kienle, Phys. Rev. B **77**, 035432 (2008).
[9] R. Dennington II, T. Keith, J. Millam, K. Eppinnett, W. L. Hovell, and R. Gilliland, GAUSSVIEW, Version 3.0, Semichem, Inc., Shawnee Mission, KS, 2003.
[10] J. Cerda and F. Soria, Phys. Rev. B **61**, 7965 (2000).
[11] H. Raza and E. C. Kan, arXiv:0803.1699v2 (unpublished).
[12] C. L. Petersen, F. Greya, I. Shiraki, and S. Hasegawa, Appl. Phys. Lett. **77**, 3782 (2000).